

This document is confidential and is proprietary to the American Chemical Society and its authors. Do not copy or disclose without written permission. If you have received this item in error, notify the sender and delete all copies.

Electronic Transition of Ferrocenium: Neon Matrix and CASPT2 Studies

Journal:	<i>The Journal of Physical Chemistry</i>
Manuscript ID	jp-2016-10391t.R1
Manuscript Type:	Special Issue Article
Date Submitted by the Author:	26-Nov-2016
Complete List of Authors:	Fulara, Jan; Polska Akademia Nauk, Institute of Physics; University of Basel, Department of Chemistry Filipkowski, Karol; University of Basel, physical chemistry Maier, John; University of Basel, Department of Chemistry

SCHOLARONE™
Manuscripts

Electronic Transition of Ferrocenium: Neon Matrix and CASPT2 Studies

Jan Fulara,^{1,2} Karol Filipkowski,¹ John P. Maier^{*,1}

¹Department of Chemistry, University of Basel, Klingelbergstrasse 80, CH-4056, Basel, Switzerland

²Institute of Physics, Polish Academy of Sciences, Al. Lotników, 32/46, PL-02-668 Warsaw, Poland

Abstract

Electronic absorptions of ferrocenium starting at 632.5 nm were measured in a 6 K neon matrix following mass – selective deposition of the ions. The spectrum shows clear vibrational structure and provides the best yet resolved view of the electronic states of this cation. The absorption system is identified as the $1^2E_1' \leftarrow X^2E_2'$ transition (D_{5h} symmetry) on the basis of vertical excitation energies and oscillator strengths calculated at the CASPT2 level. Vibrational bands in the spectrum are assigned with the aid of the ground state frequencies calculated with the DFT method.

Introduction

Ferrocene, dicyclopentadienyl iron, (FeCp_2) was discovered in the middle of the last century^{1,2} and since then was a subject of numerous experimental and theoretical studies³. Ferrocene is a stable, non-toxic, readily functionalizing compound having, in addition, a low redox potential. Due to these unique features ferrocene - based materials are of interest in electrochemistry, biology, pharmacy and materials science. They can be used as catalysts^{4,5}, biosensors⁶ or anticancer drugs^{7,8}. Ferrocenium (FeCp_2^+) plays a key role in these systems, for example it is responsible for the cytotoxic activity against cancer cells^{9,10}.

In contrast to neutral ferrocene, much less is known about its ion, although the first electronic absorption spectrum of ferrocenium was already measured in the late fifties as a charge transfer complex with iodine¹¹. Several spectroscopic studies on FeCp_2^+ in strong Lewis acids and on ferrocenium salts in solid environment¹²⁻¹⁴ have been carried out and structured absorptions starting around 630 nm were reported. The ground state of FeCp_2^+ was characterized as $^2\text{E}_{2g}$ (in D_{5d} symmetry) by electron spin resonance^{15,16}, magnetic susceptibility¹⁴ and neutron scattering studies¹⁷. Theoretical studies^{18,19} on FeCp_2^+ have revealed that the transition observed in the visible range is due to electronic excitation to the $^2\text{E}_{1u}$ state. The $^2\text{E}_{1u} \leftarrow X^2\text{E}_{2g}$ transition was studied in the gas-phase by photodissociation spectroscopy; however the resolution was poor and vibrational structure was not observed²⁰. Photoelectron studies on ferrocene give some insight on the energetics of the ground and several excited electronic states of its cation^{21,22}.

In this contribution the electronic absorption spectrum of ferrocenium in solid neon is reported and assigned to the $^2\text{E}'_1 \leftarrow X^2\text{E}'_2$ transition (D_{5h}) based on CASPT2 calculations.

Experimental

The set-up used employs mass-selected ion deposition into a 6 K neon matrix. Ferrocenium ions were produced in a hot cathode discharge from a mixture of ferrocene vapours with helium at room temperature. Ions were extracted from the source by a series of electrodes and guided into an electrostatic bender, separating neutral and ionic species. After passing through a mass filter cations were co-deposited with neon onto a rhodium-coated sapphire plate to build ~150 μm matrix over 4-5 hours. Chloromethane mixed with neon in a 1:25000 ratio was used as an electron scavenger to prevent the neutralization of trapped ions by electrons ejected from metal surfaces.

Absorption spectra were recorded by probing the matrix with broadband light from a halogen or xenon lamp, parallel to the sapphire substrate in a waveguide manner. The light transmitted through the matrix was collected by an optic-fiber bundle. Collected light illuminated the slit of 0.3 m spectrograph combined with two wavelength-specific CCD cameras. The electronic absorption spectra in the 220 – 1100 nm range were obtained by recording a series of overlapping 50 – 70 nm sections and then merging them. The measurements were started in near IR and continued towards UV using appropriate cut-off filters, to avoid neutralization or photo-conversion of trapped ions. Ions were then neutralized with UV photons ($\lambda > 260$ nm) from a medium pressure mercury lamp, and the spectrum recorded anew to distinguish the absorption of neutrals and charged species.

Computational

To assign the electronic spectrum of ferrocenium, the symmetry and excitation energy of the electronic states involved and oscillator strength were calculated by *ab initio* methods. A sufficiently large basis set for iron is needed. The Wachters+f basis set for iron^{23,24}, aug-cc-pVDZ for carbon²⁵ and hydrogen and the B3LYP functional²⁶ were used for geometry optimization. Calculations have been done with the Gaussian 09 program package²⁷. Computations at the same level for the ferrocene itself provided almost the same frequencies of the vibrational modes as in ref. 28 (Table 1SI). Two arrangements of the Cp rings: eclipsed (D_{5h}) and staggered (D_{5d}) can be distinguished, separated by a low energy barrier (~ 4 kJ/mol for the neutral)²⁸. A minimum for ferrocenium is predicted at D_{5h} symmetry. One imaginary frequency (-36 cm $^{-1}$) and a slightly higher energy (~ 1 kJ/mol) is obtained for the D_{5d} structure (Table 2SI). The coordinates of the ground electronic state computed at the DFT level of theory were used for the excitation energy and oscillator strength predictions of the D_{5h} and the D_{5d} transition state structure. For computational reasons, these were carried out using the ANO L/5s4p2d1f, ANO L/3s2p1d and ANO L/2s1p basis set for iron, carbon and hydrogen atoms, respectively and the symmetries were lowered to the C_{2v} and C_{2h} point groups. Multi-state second-order perturbation theory^{29,30} was employed, and the wavefunctions were optimized for the average energy of the four roots. Molcas 8 program³¹ was used. Eleven electrons residing on the HOMO orbitals, which belong to a_1 , b_1 , a_2 and b_2 irreducible representations of C_{2v} (the largest abelian subgroup of D_{5h}), were distributed on twelve orbitals and formed the active space in the multistate CASPT2 calculations. The orbitals and the active space are shown schematically in Fig. 1SI. The ground electronic state of ferrocenium belongs to the E'_2 irreducible representation of D_{5h} and the first excited state to the E'_2 . At the lower C_{2v} symmetry both electronic states belong to the $a_1 + b_1$ representations. The

1
2
3 energy of X $^2E'_2$ and $1^2E'_1$ states is equal to the a_1 and b_1 representations. The same is observed
4
5 for the excitation energies and the oscillator strengths (see Supporting Information for a more
6
7 extended discussion).
8
9

10 11 12 13 **Results and Discussion**

14
15
16 Deposition of ferrocene cations into solid neon resulted in strong absorptions
17
18 commencing at 632.5 nm (blue trace, Figure 1). The absorptions diminished upon UV irradiation
19
20 ($\lambda > 260$ nm) of the matrix (red trace), suggesting cationic carrier. The origin band and the next
21
22 strongest one at 621.0 nm show a triplet structure, with spacing of 25 and 63 cm^{-1} . The same
23
24 motif, although less pronounced, is seen for the other vibrational bands. The wavelength of the
25
26 origin band in solid neon (632.5 nm) lies not far from that one reported in solution (~ 635 nm)^{13,14}
27
28 or KBr pellet (around 640 nm)¹². The separation of the first two bands in the photoelectron
29
30 spectrum of ferrocene²¹ (with a typical uncertainty of ± 80 cm^{-1}) yields the wavelengths of 674 ± 4
31
32 nm for the vertical energy to the first excited electronic state and 621.5 ± 3 nm for the adiabatic
33
34 one²². Vibrational structure with a spacing of $\sim 278 \pm 80$ cm^{-1} is apparent in the photoelectron
35
36 spectrum of ferrocene²². The progression built on the same vibrational mode, 293 cm^{-1} ,
37
38 dominates the neon matrix absorption spectrum (Figure 1). The gas-phase photoelectron data to
39
40 neon matrix shift of the origin band is, in the range observed for a large number of cations³²⁻³⁴.
41
42
43
44
45

46
47 The strongest $1^2E_{1u} \leftarrow X^2E_{2g}$ electronic transition of the D_{5d} structure is predicted at 2.04
48
49 eV with an oscillator strength (f) of 0.007 and the $1^2E_1' \leftarrow X^2E_2'$ transition of the D_{5h} structure at
50
51 2.44 eV ($f=0.012$). These can be compared with the onset at 632.5 nm (1.96 eV) in solid neon.
52
53 The vertical excitation energy computed with the same basis set and a smaller active space (11
54
55 electrons distributed on 11 orbitals) is slightly larger (2.52 eV) and the respective adiabatic value
56
57
58
59
60

1
2
3 obtained is 2.31 eV. The latter computed with a larger basis set should match better the
4
5 observation.
6

7
8 Ionization of ferrocene (D_{5h}) was studied by the symmetry adapted cluster-configuration-
9
10 interaction method and energies of several excited electronic states of $FeCp_2^+$ were reported³⁵.
11
12 The ground state of the cation has $^2E_2'$ symmetry and the first electronic transition to the $1^2E_1'$
13
14 state is expected in the optical domain at 2.52 eV, close to the CASPT2 energy. The next
15
16 electronic state of the same symmetry lies at 6.37 eV. The bonding nature of the ground and
17
18 excited electronic states of $FeCp_2^+$ has also been discussed³⁵. Ferrocene is an example where
19
20 Koopmans' theorem breaks down; the ground state of $FeCp_2^+$ is formed upon removal of an
21
22 electron from the inner e_2' orbital, mainly composed of the $3d_{xy}$ and $3d_{x^2-y^2}$ atomic orbitals of
23
24 iron. The $1^2E_1'$ state is produced upon removal of an electron from the e_1' orbital, essentially the
25
26 π orbitals of Cp and 4p of iron³⁵. The present CASPT2 studies lead to the similar conclusions.
27
28
29
30
31

32 Based on the theoretical calculations, the electronic spectrum shown in Figure 1 is
33
34 assigned to the $1^2E_1' \leftarrow X^2E_2'$ electronic transition of ferrocenium (D_{5h}). The four strongest
35
36 bands in the spectrum belong to a vibrational progression with spacings $\sim 290\text{ cm}^{-1}$ (Table 1). A
37
38 similar vibrational structure was observed in frozen Lewis acids¹², KBr pellets¹⁴ and the
39
40 photoelectron spectrum of ferrocene²². The 290 cm^{-1} frequency inferred is close to 292 cm^{-1} , the
41
42 value calculated at the DFT level for the ν_4 vibration (a_1') in the ground state of the cation (Table
43
44 2SI and Fig. 2SI). ν_4 is the totally symmetric ring - metal stretch and its energy does not differ
45
46 much from the 303 cm^{-1} value observed in the Raman spectrum of the neutral ferrocene³⁶. The ν_4
47
48 fundamental forms combination bands with other vibrations (Fig. 1). Two other a_1' vibrations (ν_3
49
50 and ν_2) and their combinations with ν_4 are identified in the spectrum. The remaining bands may
51
52 result from the excitation of double quanta of non-totally symmetric vibrations and their
53
54 combinations with ν_4 or the other modes. One example of such an excitation is a weak band lying
55
56
57
58
59
60

1
2
3 216 cm^{-1} above the origin. There is no such mode in the calculated frequencies of either ferrocene
4
5 or its cation (Tables SII,2). The band appears as a double excitation of ν_{16} (e_1') with energy 112
6
7 cm^{-1} . Combinations of $2\nu_{16}$ with ν_4 are responsible for the bands lying 501 and 785 cm^{-1} above
8
9 the onset.
10

11
12 A number of possible combinations of different modes increases in short-wavelength part
13 of the spectrum and assignment given in Table 1 is tentative. The ESR^{15,16} and neutron
14
15 scattering¹⁷ studies show that the degenerate ground state of ferrocenium splits into two
16
17 components around 515 cm^{-1} apart due to spin – orbit coupling and a Jahn –Teller distortion.³⁷
18
19 The $1^2E_1'$ electronic state also separates into a doublet and transitions to the two components are
20
21 observed in the magnetic circular dichroism¹⁸ (500 cm^{-1}) and gas – phase photodissociation²⁰
22
23 ($\sim 600 \text{ cm}^{-1}$) spectra of ferrocene cation.. However the resolution in the latter case was very low.
24
25 Thus the band lying 501 cm^{-1} above the origin in absorption spectrum of ferrocene cation in neon
26
27 could be the origin to the second doublet of the $1^2E_1'$ state. At 6 K only electronic transitions
28
29 from the lowest energy component of the X^2E_2' doublet are observed. Some weak bands above
30
31 613.1 nm may belong to the electronic transition of the second doublet component of the
32
33 $1^2E_1'$ state.
34
35
36
37
38
39
40
41
42

43 Conclusions

44
45
46 The present study provides the best vibrationally resolved electronic absorption spectrum of
47
48 ferrocenium to date. It was obtained in a 6 K neon matrix following deposition of mass –
49
50 selected ions. The absorptions starting at 632.5 nm are assigned to the $1^2E_1' \leftarrow X^2E_2'$ electronic
51
52 transition on the basis of CASPT2 calculations. The strongest bands in the spectrum are due to
53
54
55
56
57
58
59
60

1
2
3 vibrational excitations involving the ν_4 - ring to metal stretching mode. The neon matrix spectrum
4
5 provides the basis for gas-phase measurements of this cation in the future.
6
7
8
9

10 **Author Information**

11
12 *E-mail: j.p.maier@unibas.ch. Phone: +41 (0)61 267 38 26.
13
14

15 **Acknowledgement**

16
17 This work was supported by the Swiss National Science Foundation.
18
19
20
21
22
23
24
25
26
27

28 **Supporting Information Description**

- 29
30 - Extended discussion on the CASPT2 calculations
31
32 - Most significant configurations of ferrocenium, predicted by Molcas 8 program.
33
34 - Figure showing HOMO-LUMO orbitals of ferrocenium cation (D_{5h})
35
36 - Figure of ν_4 normal mode
37
38 - Comparison of ground state vibrational frequencies of neutral ferrocene (D_{5h}) calculated
39
40 with the DFT method and reference values from ref. 28.
41
42 - Comparison of ground state vibrational frequencies of neutral D_{5h} and D_{5d} ferrocene
43
44 cation calculated with the DFT method.
45
46
47
48
49
50
51
52
53
54
55
56
57
58
59
60

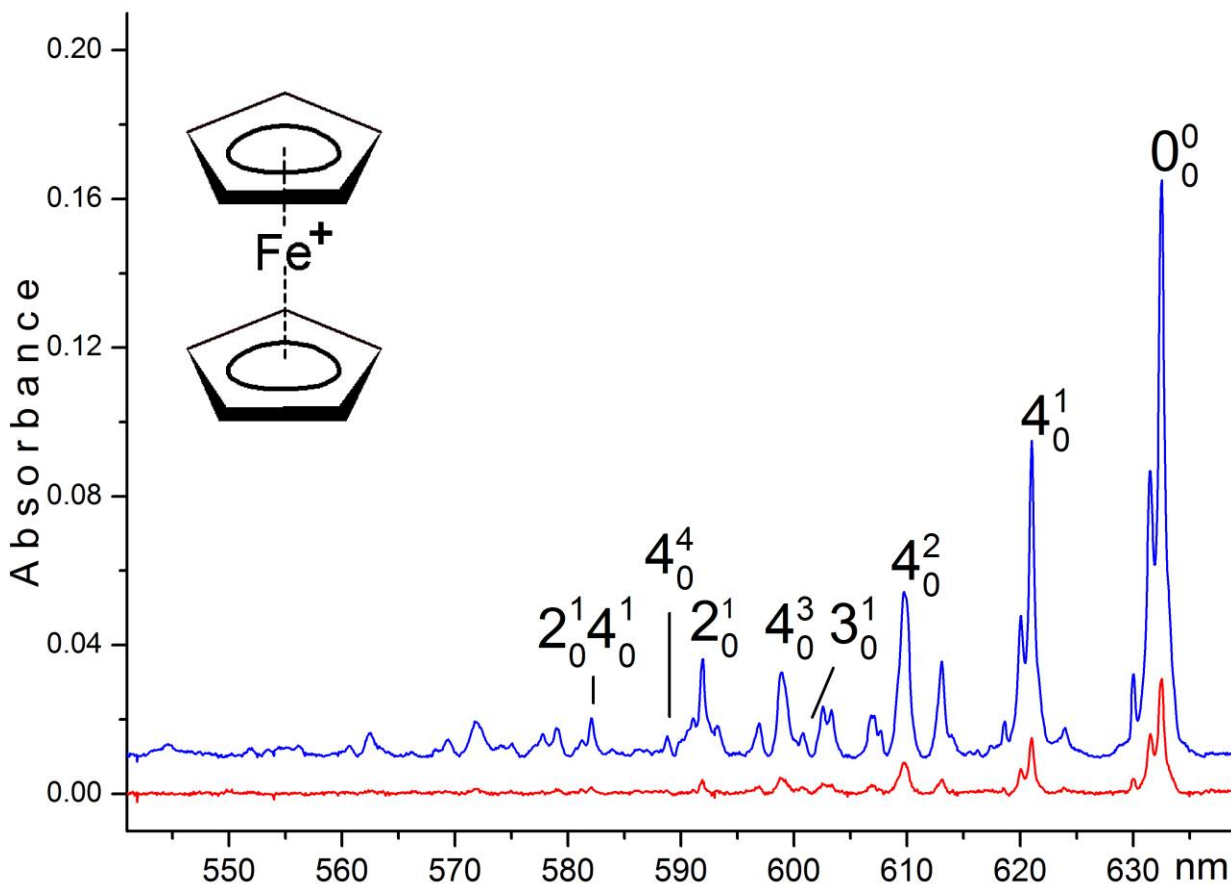


Figure 1 $1^2E'_1 \leftarrow X^2E'_2$ electronic absorption spectrum of ferrocenium ion (D_{5h}) in a 6 K neon matrix containing a trace of CH_3Cl , together with proposed assignments (blue trace). The red trace was recorded after irradiation with $\lambda > 260$ nm photons.

Table 1. Observed band maxima (± 0.1 nm) in the absorption spectrum of ferrocenium (D_{5h} symmetry) in a 6 K neon matrix. The assignment is based on electronic excitation energy computed with the CASPT2 method and vibrational frequencies calculated for the ground electronic state, with DFT (Table 2SI).

λ /nm	$\tilde{\nu}$ /cm ⁻¹	Δ /cm ⁻¹	Assignment
632.5	15810	0	$0_0^0 \ 1 \ ^2E_1' \leftarrow X \ ^2E_2'$
624.0	16026	216	$2\nu_{16}$
621.0	16103	293	ν_4
613.1	16311	501	$\nu_4 + 2\nu_{16}$ or ^{a)} 0_0^0
609.7	16402	592	$2\nu_4$
606.8	16480	670	$2\nu_{22}$
603.3	16576	766	$2\nu_{15}$
602.6	16595	785	$2\nu_4 + 2\nu_{16}$
600.8	16644	834	ν_3
598.9	16697	887	$3\nu_4$
596.9	16753	943	
593.2	16858	1048	$2\nu_{15} + \nu_4$
591.9	16895	1085	ν_2
588.8	16984	1174	$4\nu_4$
582.1	17179	1369	$\nu_2 + \nu_4$
579.1	17268	1458	
577.7	17310	1500	$4\nu_{15}$
571.8	17489	1679	
569.4	17562	1752	$1458 + \nu_4$
562.4	17781	1971	$1679 + \nu_4$
560.7	17835	2025	
544.6	18362	2552	

^{a)} The origin of the electronic transition to the second Jahn-Teller component of the $1 \ ^2E_1'$ state.

References

- ¹ Kealy, T. J.; Pauson, P. L. A New Type of Organo-Iron Compound. *Nature*. **1951**, *168*, 1039-1040.
- ² Millers, S.A.; Tebboth, J.A.; Tremaine, J. F. Dicyclopentadienyliron . *J. Chem. Soc.* **1952**, 632-635.
- ³ Adams, R.D. (2001) Special Issue: 50th Anniversary of the Discovery of Ferrocene. *J. Organomet. Chem.* **2001**, 637–639.
- ⁴ Atkinson, R. C. J.; Gibson V. C.; Long, N. J. The Syntheses and Catalytic Applications of Unsymmetrical Ferrocene Ligands. *Chem. Soc. Rev.* **2004**, *33*, 313-328.
- ⁵ Shafir, A.; Arnold, J. Ferrocene-Based Olefin Polymerization Catalysts: Activation, Structure, and Intermediates. *Organometallics*, **2003**, *22*, 567–575.
- ⁶ Sun, R.; Wang, L.; Yu, H.; Abdin, Z.-ul; Chen, Y.; Huang, J.; Tong, R. Molecular Recognition and Sensing Based on Ferrocene Derivatives and Ferrocene-Based Polymers. *Organometallics* **2014**, *33*, 4560–4573.
- ⁷ Braga, S. S.; Silva, A. M. S. A New Age for Iron: Antitumoral Ferrocenes. *Organometallics* **2013**, *32*, 5626–5639.
- ⁸ Fouda, M. F. R.; Abd-Elzaher, M. M.; Abdelsamaia, R. A.; Labib, A. A. On the Medicinal Chemistry of Ferrocene. *Appl. Organometal. Chem.* **2007**, *21*, 613–625.
- ⁹ Köpf-Maier, P.; Köpf, H.; Neuse, E. W. Ferrocenium Salts—the First Antineoplastic Iron Compounds. *Angew. Chem., Int. Ed. Engl.* **1984**, *23*, 456–457.
- ¹⁰ Houlton, A.; Roberts, R.M.G.; Silver, J. Studies on the Anti-Tumour Activity of Some Iron Sandwich Compounds. *J. Organomet. Chem.* **1991**, *418*, 107–112.
- ¹¹ Brand, J. C. D.; Snedden, W.; Electron-Transfer Spectra of Ferrocene. *Trans. Faraday Soc.* **1957**, *53*, 894-900.

1
2
3
4
5
6
7
8
9
10
11
12
13
14
15
16
17
18
19
20
21
22
23
24
25
26
27
28
29
30
31
32
33
34
35
36
37
38
39
40
41
42
43
44
45
46
47
48
49
50
51
52
53
54
55
56
57
58
59
60

¹² Sohn, Y. S.; Hendrickson, D. N.; Gray, H. B. Electronic Structure of Ferricenium Ion. *J. Am. Chem. Soc.* **1970**, *92*, 3233-3234.

¹³ Sohn, Y. S.; Hendrickson, D. N.; Gray, H. B. Electronic Structure of Metallocenes *J. Am. Chem. Soc.* **1971**, *93*, 3603-3612.

¹⁴ Hendrickson, D. N.; Sohn, Y. S.; Duggan D. M.; Harry, B. G. Low-Temperature (4.2 °K) Study of the ${}^2E_{1u} \leftarrow {}^2E_{2g}$ Band System in the Electronic Spectra of Various Ferricinium Compounds. *J. Chem. Phys.* **1973**, *58*, 4666-4675.

¹⁵ Prins, R.; Reinders, F. J. Electron Spin Resonance of the Cation of Ferrocene *J. Am. Chem. Soc.* **1969**, *91*, 4929-4931.

¹⁶ Prins, R. Electronic Structure of the Ferricenium Cation; Electron Spin Resonance Measurements of the Cations of Ferrocene Derivatives. *Mol. Phys.* **1970**, *19*, 603-620.

¹⁷ Kemner, E.; de Schepper, I. M.; Kearley, G. J. The Vibrational Spectrum of Solid Ferrocene by Inelastic Neutron Scattering. *J. Chem. Phys.* **2000**, *112*, 10926-10929.

¹⁸ Rowe, M. D.; McCaffery, A. J. Electronic Structure of Ferricenium Ion from Absorption, MCD, and ESR Studies. *J. Chem. Phys.* **1973**, *59*, 3786-3794

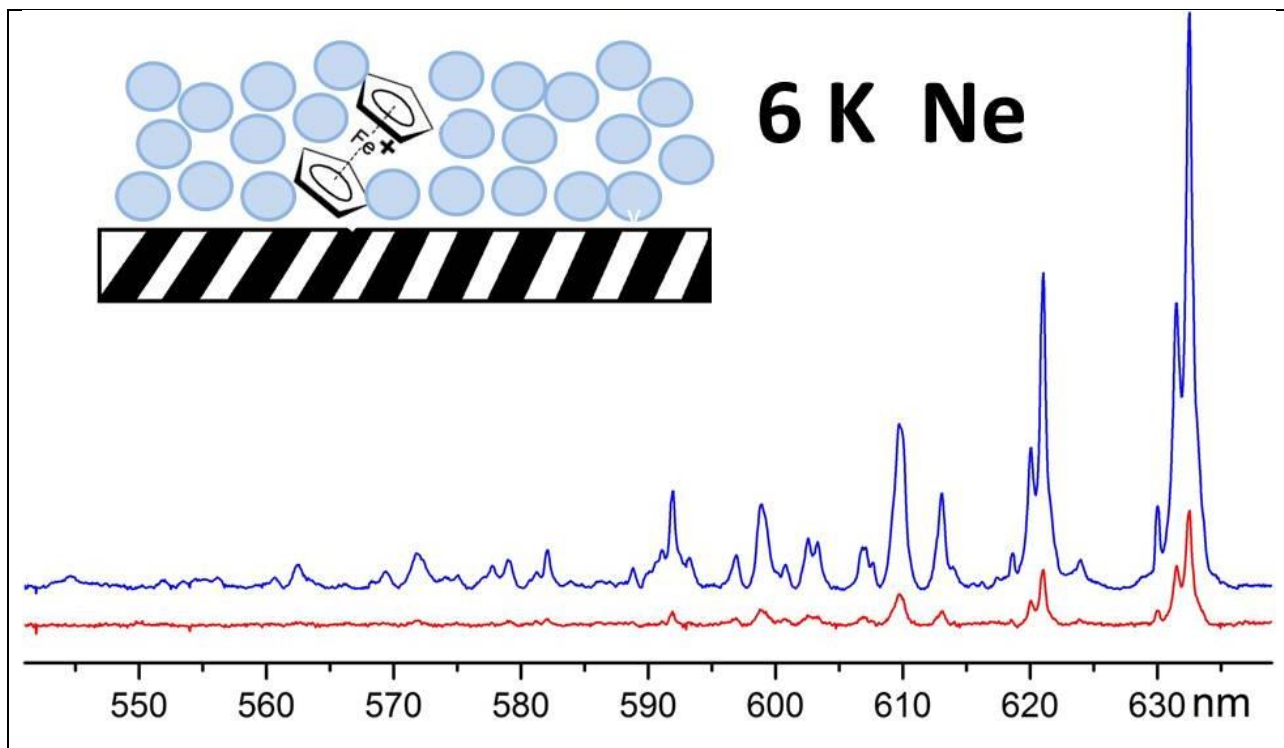
¹⁹ Bagus, P. S.; Walgren U. I.; Almlöf J. A Theoretical Study of the Electronic Structure of Ferrocene and Ferricinium: Application to Mössbauer Isomer Shifts, Ionization Potentials, and Conformation. *J. Chem. Phys.* **1976**, *64*, 2324-2334.

²⁰ Faulk, J. D.; Dunbar R. C. Photodissociation Spectroscopy of Gas-Phase Ferrocene Cation. *J. Am. Soc. Mass. Spectrom.* **1991**, *2*, 97-102.

²¹ Evans, S.; Green, M. L. H.; Jewitt, B.; King, G. H.; Orchard, A. F. Electronic Structures of Metal Complexes Containing the π -Cyclopentadienyl and Related Ligands. Part 2.—He I Photoelectron Spectra of the Open-Shell Metallocenes. *J. Chem. Soc. Faraday II* **1974**, *70*, 356-376.

- 1
2
3
4
5
6
7
8
9
10
11
12
13
14
15
16
17
18
19
20
21
22
23
24
25
26
27
28
29
30
31
32
33
34
35
36
37
38
39
40
41
42
43
44
45
46
47
48
49
50
51
52
53
54
55
56
57
58
59
60
-
- ²² Rabalais, J. W.; Werme, L. O.; Bergmark, T.; Karlsson, L.; Hussain, M.; Siegbahn K. Electron Spectroscopy of Open - Shell Systems: Spectra of Ni(C₅H₅)₂, Fe(C₅H₅)₂, Mn(C₅H₅)₂, and Cr(C₅H₅)₂. *J. Chem. Phys.* **1972**, *57*, 1185-1192.
- ²³ Feller, D. The Role of Databases in Support of Computational Chemistry Calculations. *J. Comp. Chem.* **1996**, *17*, 1571-1586.
- ²⁴ Schuchardt, K. L.; Didier, B. T.; Elsethagen, T.; Sun, L.; Gurumoorthi, V.; Chase, J.; Li, J.; Windus, T.L. Basis Set Exchange: A Community Database for Computational Sciences. *J. Chem. Inf. Model.* **2007**, *47*, 1045-1052.
- ²⁵ Dunning, T. H. Jr. Gaussian Basis Sets for use in Correlated Molecular Calculations. I. The Atoms Boron through Neon and Hydrogen. *J. Chem. Phys.* **1989**, *90*, 1007-1023.
- ²⁶ Lee, C.; Yang, W.; Parr, R. G.; Development of the Colle-Salvetti Correlation-Energy Formula into a Functional of the Electron Density. *Phys. Rev.* **1988**, *B 37*, 785-789.
- ²⁷ Gaussian 09, Revision D.01, Frisch, M. J.; Trucks, G. W.; Schlegel, H. B.; Scuseria, G. E.; Robb, M. A.; Cheeseman, J. R.; Scalmani, G.; Barone, V.; Mennucci, B.; Petersson, G.; et. al. Gaussian, Inc., Wallingford CT, 2009.
- ²⁸ Xu, Z.- F.; Xie, Y.; Feng, W.-L.; Schaefer, H. F. III. Systematic Investigation of Electronic and Molecular Structures for the First Transition Metal Series Metallocenes M(C₅H₅)₂ (M =V, Cr, Mn, Fe, Co, and Ni). *Phys. Chem. A* **2003**, *107*, 2716-2729.
- ²⁹ Andersson, K.; Malmqvist, P.-Å.; Roos, B. O.; Sadlej, A. J.; Wolinski, K. Second-Order Perturbation Theory with a CASSCF Reference Function. *J. Phys. Chem.* **1990**, *94*, 5483-5488.
- ³⁰ Andersson, K.; Malmqvist, P.-Å.; Roos, B. O. Second-Order Perturbation Theory with a Complete Active Space Self-Consistent Field Reference Function. *J. Chem. Phys.* **1992**, *96*, 1218-1226.
- ³¹ Aquilante, F.; De Vico, L.; Ferré, N.; Ghigo, G.; Malmqvist, P.-Å.; Neogrády, P.; Pedersen, T.B.; Pitonak, M.; Reiher, M.; Roos, B.O. et al. *Comp. Chem.* **2010**, *31*, 224-247.

- 1
2
3
4
5
6
7
8
9
10
11
12
13
14
15
16
17
18
19
20
21
22
23
24
25
26
27
28
29
30
31
32
33
34
35
36
37
38
39
40
41
42
43
44
45
46
47
48
49
50
51
52
53
54
55
56
57
58
59
60
-
- ³² Campos, F. X.; Jiang, Y.; Grant, E. R. Triple-Resonance Spectroscopy of the Higher Excited States of NO₂. II. Vibrational Mode Selectivity in the Competition Between Predissociation and Autoionization. *J. Chem. Phys.* **1990**, *93*, 7731-7739
- ³³ Weaver, A.; Arnold, D. W.; Bradforth, S. E. Examination of the ²A'₂ and ²E' States of NO₃ by Ultraviolet Photoelectron Spectroscopy of NO₃⁻. *J. Chem. Phys.* **1991**, *94*, 1740-1751.
- ³⁴ Warren, D. F.; Thompson, W. E.; Jacox, M. E. The Vibrational Spectra of Molecular Ions Isolated in Solid Neon. XI. NO₂⁺, NO₂⁻, and NO₃⁻. *J. Chem. Phys.* **1993**, *99*, 7393-7402
- ³⁵ Ishimura, K.; Hada, M.; Nakatsuji, H. Ionized and Excited States of Ferrocene: Symmetry Adapted Cluster–Configuration–Interaction Study. *J. Chem. Phys.* **2002**, *117*, 6533-6537.
- ³⁶ Lippincott, E. R.; Nelson, R. D. The Vibrational Spectra and Structure of Ferrocene and Ruthenocene. *Spectrochim. Acta*, **1958**, *10*, 307-329.
- ³⁷ Stebler, A.; Furrer, A.; Ammeter, J. H. Direct Observation of the Ground-State Splitting in d⁵ and d⁷ Metallocenes by Inelastic Neutron Scattering. *Inorg. Chem.* **1984**, *23*, 3493–3500.



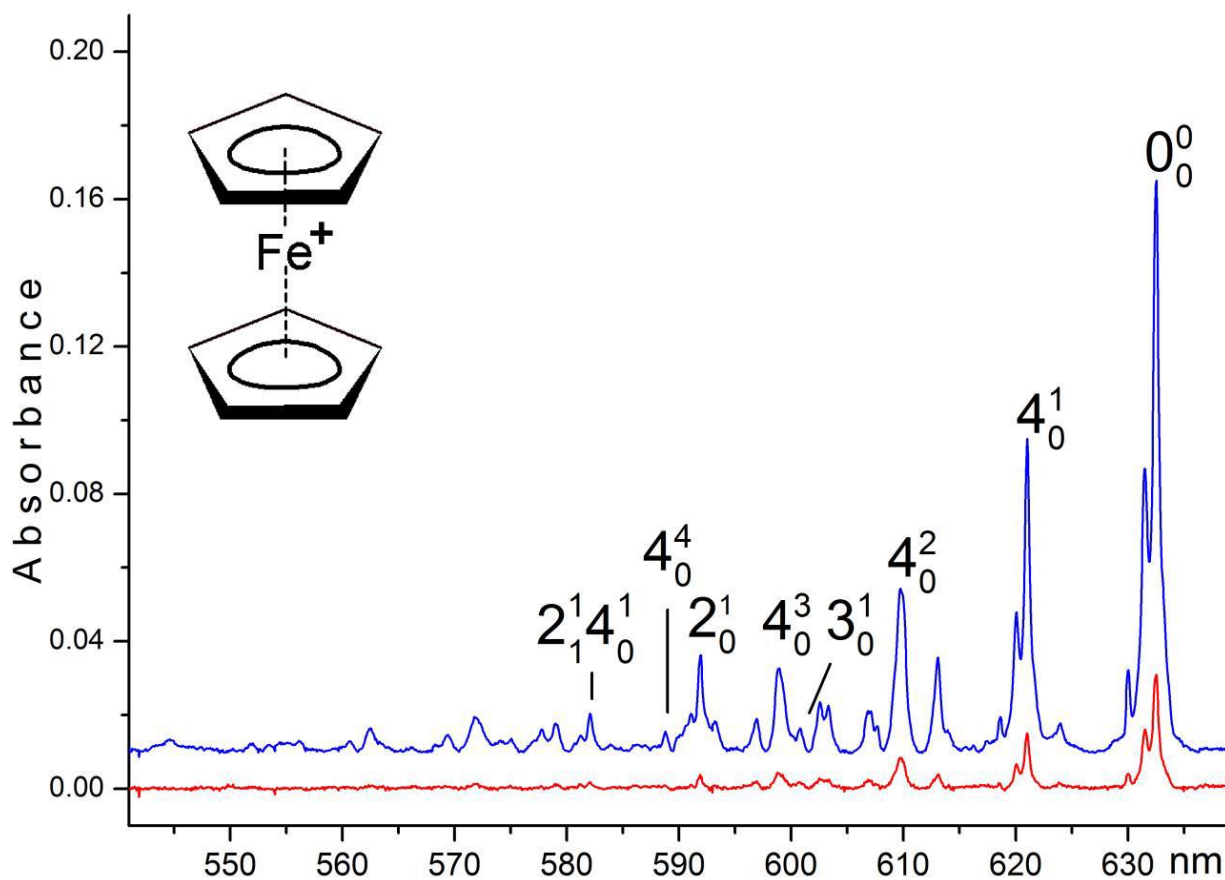


Figure 1 $1^2E'_1 \leftarrow X^2E'_2$ electronic absorption spectrum of ferrocenium ion (D_{5h}) in a 6 K neon matrix containing a trace of CH_3Cl , together with proposed assignments (blue trace). The red trace was recorded after irradiation with $\lambda > 260$ nm photons.